Defect and Diffusion Forum
ISSN: 1662-9507, Vol. 450, pp 49-59
doi:10.4028/p-YtwNQ4

Submitted: 2026-01-12
Revised: 2026-02-19
Accepted: 2026-02-22
Online: 2026-04-15

Potential of Cutting Fluid Application in Gear Hobbing of High-Strength Materials

Martin Beutner[1,a*], Matthias Hackert-Oschätzchen[1,b], Marco Eich[2,c], Bernhard Karpuschewski[2,d]

[1]Chair of Manufacturing Technology with Focus Machining, Faculty of Mechanical Engineering, Otto von Guericke University Magdeburg, Universitätsplatz 2, 39106 Magdeburg, Germany

[2]Leibniz-Institut für Werkstofforientierte Technologien – IWT, Badgasteiner Str. 3 28359 Bremen

[a]martin.beutner@ovgu.de, [b]matthias.hackert-oschaetzchen@ovgu.de, [c]eich@iwt-bremen.de, [d]karpuschewski@iwt-bremen.de (*corresponding author)

Keywords: gear hobbing, wear, cutting fluid

Abstract. Geared components increasingly require higher torque density, driving the use of high-strength steels and necessitating stable machining processes, particularly in small and medium-sized enterprises that rely on cutting fluids. This study evaluates the performance potential of various cutting fluids in gear hobbing using a fly-cutting analogy test setup, which enables controlled and reproducible analysis of wear mechanisms of a single hob tooth. Water-based and oil-based cutting fluids, different tool substrate materials (PM-HSS, MC90, and tungsten carbide), and workpiece steels of different strength levels were systematically investigated. The results show that PM-HSS is unsuitable for machining the highest-strength material. Dry machining improved tool life, whereas the application of cutting fluids led to increased tool wear.

Introduction

Previous work conducted within the FVA (ForschungsVereinigung Antriebstechnik or Research Association for Drive Technology in Germany) research project 744 I (IGF No. 18538 BG) demonstrated that the application of different coolant-lubricant strategies in gear hobbing leads to significant variations in process performance. The investigations examined two oil-based cutting fluids, an emulsion, and dry machining, using single-tooth fly cutting as an analogy process to gear hobbing. The cutting speed v_c was varied across five levels while all remaining parameters were kept constant. Although no performance differences were observed between the two oil-based cutting fluids, dry machining exhibited substantially longer tool life at low cutting speeds. With increasing cutting speed, tool life converged toward the levels achieved with the oil-based fluids. These results were confirmed independently in Bremen and in Magdeburg, with no significant deviations between the two research institutions [1].

While these initial experiments were carried out on the case-hardening steel 20MnCrB5 with a tensile strength of $R_m \approx 530$ N/mm², the industrial relevance lies in assessing whether these findings can be transferred to the machining of higher-strength steels ($R_m \geq 1000$ N/mm²), as the torque density of modern gear systems continues to increase. Of particular interest is the technological and economic potential of wet machining compared to dry machining. Over the past two decades, research has predominantly focused on the introduction [2, 3] and further development of dry machining [4, 5, 6, 7]. However, the advantages of dry machining - such as reduced machining costs and increased productivity - are typically realized only in large-scale production [8]. In contrast, wet machining remains common in small- and medium-batch manufacturing [1], where its robustness under frequently changing gear geometries is considered beneficial.

Given this situation, no systematic studies currently exist that evaluate the potential of coolant-lubricant applications in gear hobbing of higher-strength materials while considering modern tool and machine concepts. To determine the transferability of the findings from the previous project to these more demanding material classes, further research activities are required.

Experimental Methodology

For the experimental investigations, a representative spur gear geometry from the heavy commercial vehicle (HCV) segment was selected. The experiments were conducted using the single-tooth fly cutting test (see Figure 1 b), a research-established analogy test for industrial gear hobbing, in which only a single cutting tooth is engaged in the cutting process. This approach allows a significant reduction in experimental time and cost, particularly for wear investigations, compared to full-scale gear hobbing operations [9,10]. Compared to industrial gear hobbing the process kinematic is adapted, but the resulting gear geometry is the same for both processes. Each parameter test was carried out once within this study, as preliminary three repeat experiments demonstrated stable and reproducible results regarding wear pattern and tool life, rendering further repetitions unnecessary. Due to the number of experimental combinations, the specific parameter combinations of tool substrate to the respective workpiece material are introduced in the results section.

The investigated spur gear geometry is shown in Figure 1 and is characterized by a module of 4 mm, 26 teeth and a pressure angle of 20°. The gear has an outside diameter of 114.6 mm and a face width of 60 mm, which are representative dimensions for gears used in heavy commercial vehicle applications. All experiments were carried out on a Liebherr LC 180 gear hobbing machine. The applied teeth were cut out by wire erosion from three different hobs having 18 gashes and an outer diameter of 100 mm, featuring AlCr-based coatings. The different tool substrate materials are powder metallurgical high-speed steel (PM-HSS), MC90 (an iron-based tool steel of the Fe–Co–Mo alloy system) and tungsten cemented carbide. In addition to the geometric and tool-related parameters, Figure 1 also illustrates the reference profile geometry, as well as the experimental setup on the machine tool showing the single-tooth engagement between tool and workpiece.

a)

workpiece			
module	m_n	4	mm
no. of teeth	z_2	26	
Pressure angle	α	20	°
helix angle	β	0	°
outer diameter	d_a	114.6	mm
face width	b	60	mm
tool			
substrate	PM-HSS, MC90, carbide		
coating	Al,Cr-based		
no. of. starts	z_0	1	right
lead angle	γ	2.55	°
no. of gashes	i	18	
outer diameter	d_a	100	mm

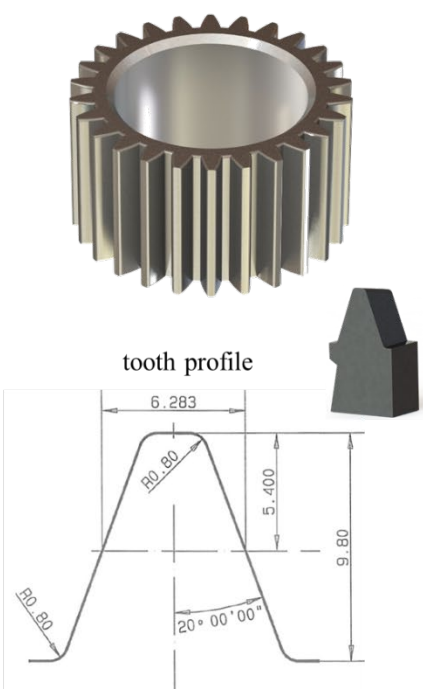

Fig. 1. a) Parameters of the gearing and b) Test setup at the machine tool

At the beginning of the investigations, the initial condition of the fly cutting teeth (with coating) was characterized measuring the surface topography of the rake face. The surface roughness was quantified using the Rz parameter, as depicted in Figure 2. Among the investigated tool substrates, the PM-HSS exhibited the highest roughness with approximately Rz ≈ 2.0 µm. In contrast, the surface roughness decreased to about Rz ≈ 1.5 µm for the MC90 substrate and further to Rz ≈ 0.5 µm for the tungsten-cemented carbide. These variations in initial surface characteristics can be attributed to the different manufacturing processes of the substrates. All recorded roughness values are within typical

industrial tolerance limits, thereby ensuring that the tools used in the experiments are representative for industrial machining conditions.

Additionally, the cutting-edge radius was examined. The cutting-edge radius at the tip of the tooth was found to be comparable for all three substrates, with in the range of $r_\beta \approx 15$ µm.

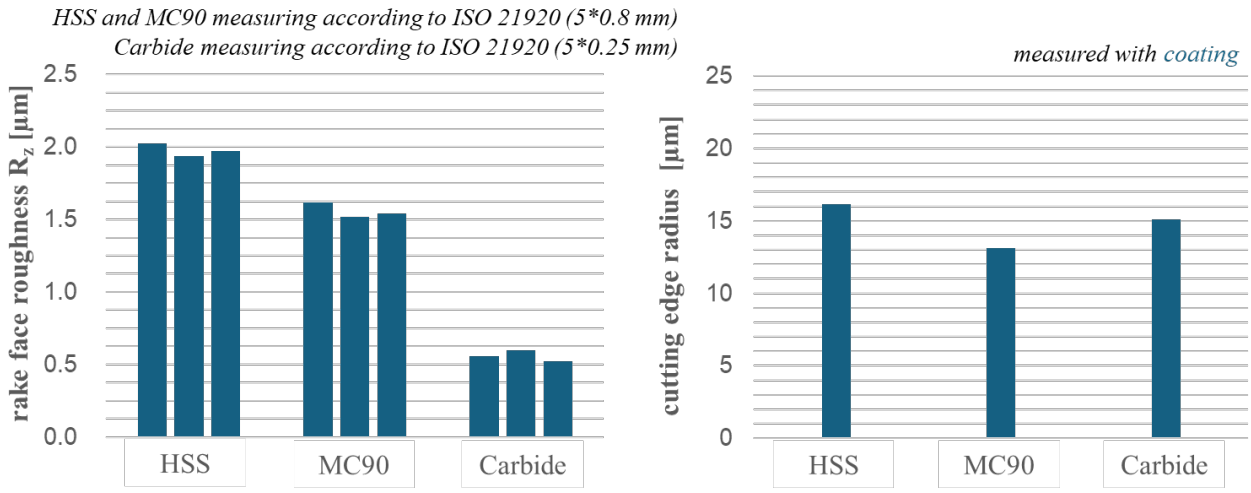

Fig. 2. Initial state of different tool substrate teeth

Table 1 and Table 2 presents the chemical composition and mechanical classification of the investigated steels, as determined by Atomic Emission Spectroscopy (AES). As a representative of application-oriented engineering steels, a quenched and tempered 42CrMoS4 (1.7227) steel was selected and investigated in two different tempering conditions in order to represent two distinct strength levels. As a representative material for the automotive sector, the case-hardening steel 20MnCrB5 (1.7168) was chosen. The chemical compositions of both steels are shown in Table 1 and Table 2.

Table 2 Chemical composition of quenched and tempered steel using atomic emission spectroscopy

1.7227 - quenched and tempered steel with Rm = 1130 N/mm² and 883 N/mm²									
C % 0.43	Mn % 0.79	Si % 0.288	Cr % 1.15	Ni % 0.05	Mo % 0.189	Cu % 0.04	P % 0.018	S % 0.022	Al % 0.035

Table 3 Chemical composition of the case-hardening steel using atomic emission spectroscopy

1.7168 - case-hardening steel with Rm = 540 N/mm²									
C % 0.150	Mn % 1.27	Si % 0.25	Cr % 1.36	Ni % 0.09	Mo % 0.05	Cu % 0.11	P % 0.009	S % 0.021	Al % 0.039

The steel grade 1.7227 exhibits a tensile strength (Rm) between Rm = 883N/mm² and Rm = 1130 N/mm², depending on the tempering condition. The steel grade 1.7168 shows a significantly lower core tensile strength of approximately Rm = 540 N/mm², which is characteristic for case-hardening steels. The low carbon content (0.15 wt.%) enables surface carburizing.

Results

Figure 3 shows the results of the interpenetration simulations performed to localize the specific load distribution along the cutting edge for the investigated gear hobbing process. The simulations were carried out using the commercial Software SpartaPro (WZL Aachen) which is used in research and industry [11,12]. Three different axial feeds (f_a = 2.9, 4.8, and 6.4 mm/rev) were calculated, while

all remaining process parameters were kept constant. The load evaluation is plotted along the unfolded tool profile, enabling a direct assignment of local load maxima along the cutting edge. The diagram a) presents the maximum uncut chip thickness as a function of the unfolded tool profile. Independent of the applied axial feed, a peak is observed at the transition between the leading flank (LF) and the tip of the tooth. Increasing the axial feed results in a systematic increase of the maximum chip thickness, while the position of the peak remains unchanged. The diagram b) shows the accumulated cutting length, revealing a similar distribution with maximum values in the transition from tip to trailing flank (TF) region. The diagram c) depicts the number of cutting engagements, again showing pronounced maxima at the identical cutting edge location as the max. uncut chip thickness. The coincidence of peak values across all evaluated load indicators confirms this region as the most highly stressed section of the cutting edge under the investigated conditions.

The microscopic image in Figure 3 shows a microscopic view of the rake face of a single hob tooth after a preliminary cutting test. The extension of the dashed vertical lines to the microscopic picture marks the critical section of the cutting edge where the load parameters reach their maximum on a worn-out tooth. This region corresponds to the geometric simulation. Local edge chipping and material breakouts on the rake face are clearly visible predicted by the simulation, showing a qualitative correlation between the simulation-based load localization and experimentally observed wear initiation.

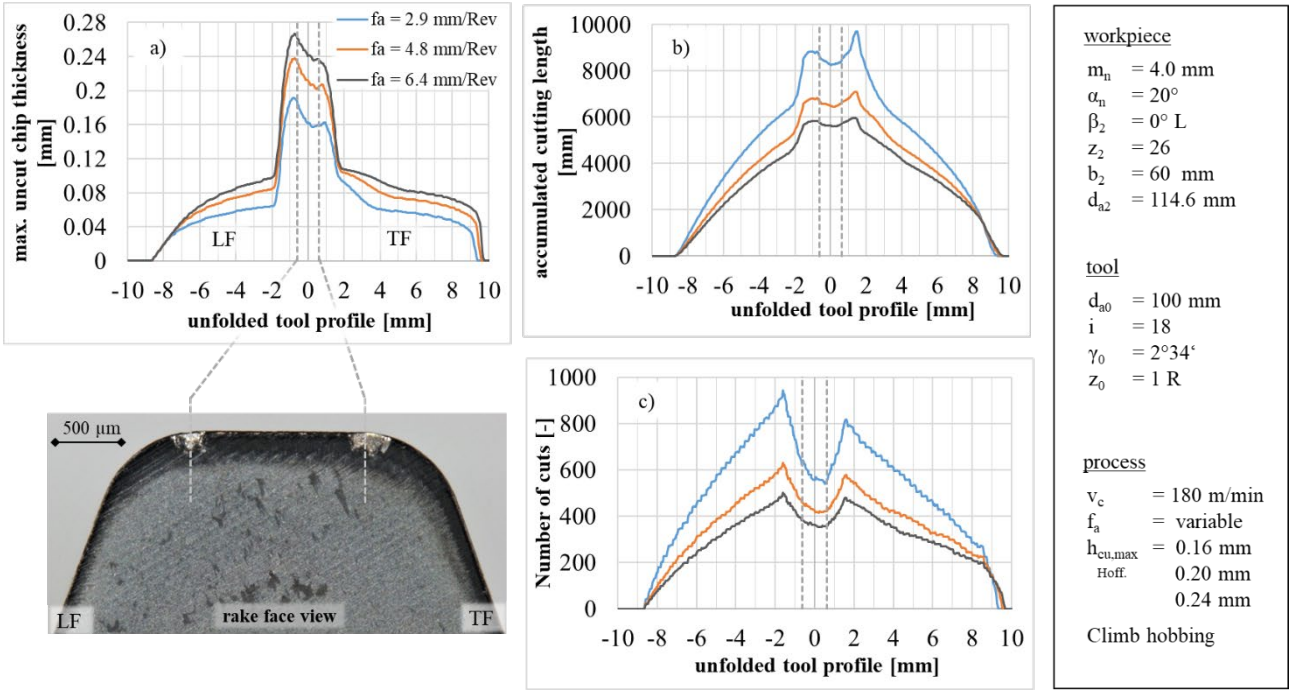

Fig. 3. Different load parameters calculated by interpenetration simulation SPARTpro:

Figure 4 a) and b) illustrates characteristic failure modes observed during preliminary cutting experiments using different coolant–lubricant strategies. A non-water-miscible metalworking fluid with a viscosity of 13 mm²/s at 40 °C and a water-miscible metalworking fluid with a concentration of 10 % were applied. Independent of the coolant–lubricant variant and despite variations in cutting parameters, the PM-HSS tool substrate proved unsuitable for machining the high-strength 42CrMoS4 steel (Rm ≈ 1130 N/mm²).

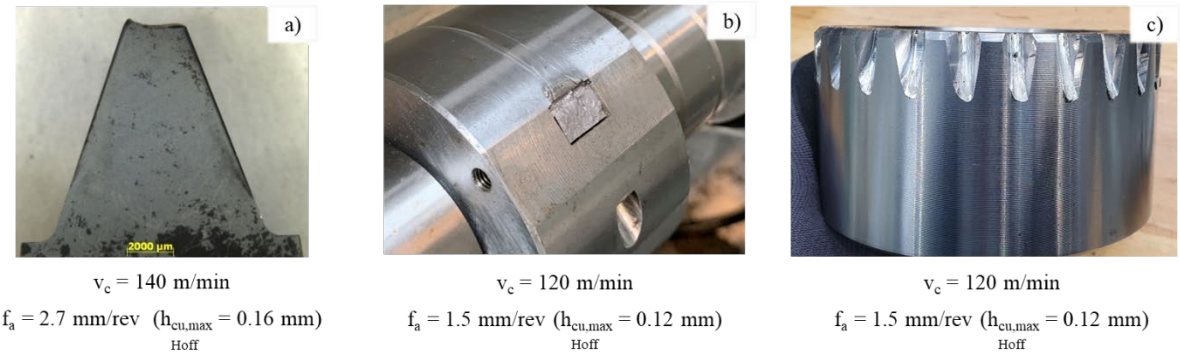

Fig. 4. a) and b) tool failure of the substrate PM-HSS for hobbing QT steel with Rm ≈ 1130 N/mm², c) resulting workpiece

Figure 4 a) shows a microscopic view of a single tooth after a short cutting time, revealing catastrophic tooth failure at the tip radius. Pronounced material breakouts and crack initiation at the cutting edge indicate excessive mechanical loading exceeding the fracture toughness of the PM-HSS substrate. Figure 4 b) depicts a failure at the tool clamping region, where the tooth fractured close to the tool body shortly after the start of the cutting process. The resulting gear is shown in Figure 4 c).This failure mode suggests high bending and impact loads acting on the tooth during interrupted cut. Due to the early occurrence of tool breakage, a further reduction of cutting parameters was not pursued, as this would have led to impractically long process times.

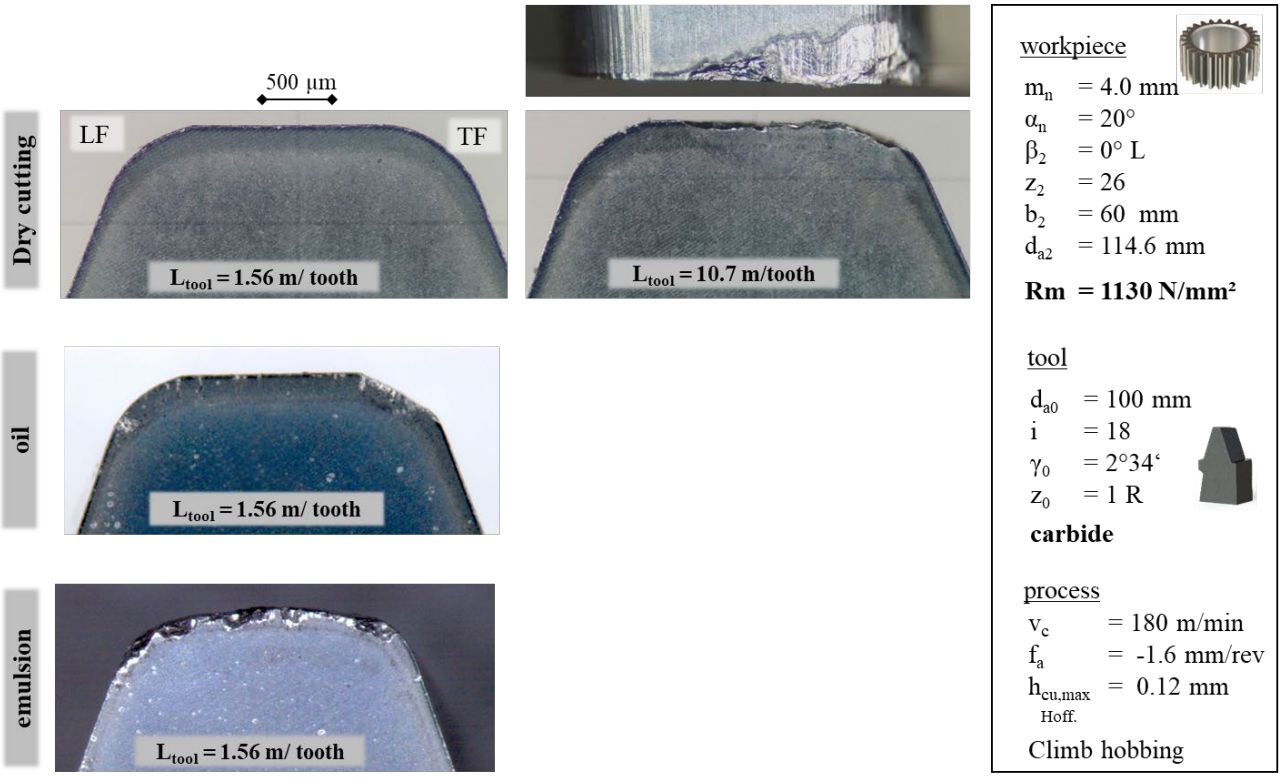

Fig. 5. Rake face comparison of the of tungsten cemented carbide substrate cutting Q&T steel with Rm ≈ 1130 N/mm²

Overall, the preliminary experiments demonstrates that, under the investigated process conditions, PM-HSS tools are not capable of reliably machining high-strength quenched and tempered 42CrMoS4 steel, regardless of the applied coolant–lubricant strategy. The observed failure modes underline the necessity of alternative tool substrates for this application.

As shown in Figure 5, dry cutting exhibits a stable wear behavior during the initial cutting stage. After machining one gear, corresponding to a cutting length of L_{tool} = 1.56 m/tooth, almost no flank wear is observed, with the flank wear land width (VB) remaining below 30 µm along the entire cutting

edge. In contrast, when applying oil or emulsion, severe edge chipping and large-scale cutting edge breakouts occur already at the same cutting length, preventing any further machining under these conditions. Consequently, both coolant–lubricant strategies lead to premature catastrophic failure of the tungsten cemented carbide tool. Dry cutting could be continued up to a tool life of L_{tool} = 10.7 m/tooth, as depicted in Figure 5 (upper right). At this cutting length, a pronounced breakout occurs at the tip flank of the tooth, resulting in a sudden increase in VB. The defined wear criterion of VB = 140 µm is exceeded, leading to the end of the experiment. This abrupt increase in flank wear is a well-known characteristic wear behavior of cemented carbide tools in gear hobbing.

To further analyze the underlying damage mechanisms, a SEM investigation was conducted on single-tooth used in dry cutting and cutting with oil, as shown in Figure 6. The SEM images of the dry-cutting condition part a) reveal locally confined substrate cracks in the vicinity of the cutting edge. However, these cracks do not exhibit the typical morphology of comb cracks [13,14], which usually develop perpendicular to the cutting edge in cemented carbide tools during gear hobbing. Moreover, no material breakout originates from these cracks, and they are therefore not considered to be tool-life determining under dry cutting conditions. In contrast, the SEM analysis of the cutting edge subjected to oil lubrication part b) shows pronounced material spalling and breakouts on the rake face, occurring perpendicular to the cutting edge. Interestingly, higher-magnification SEM images reveal that these breakouts are not associated with pre-existing substrate cracks. This observation suggests that the failure mechanism is not driven by classical comb crack propagation but is more likely related to thermally induced stresses, potentially caused by thermal shock effects due to the intermittent cooling of the cutting edge by the coolant–lubricant.

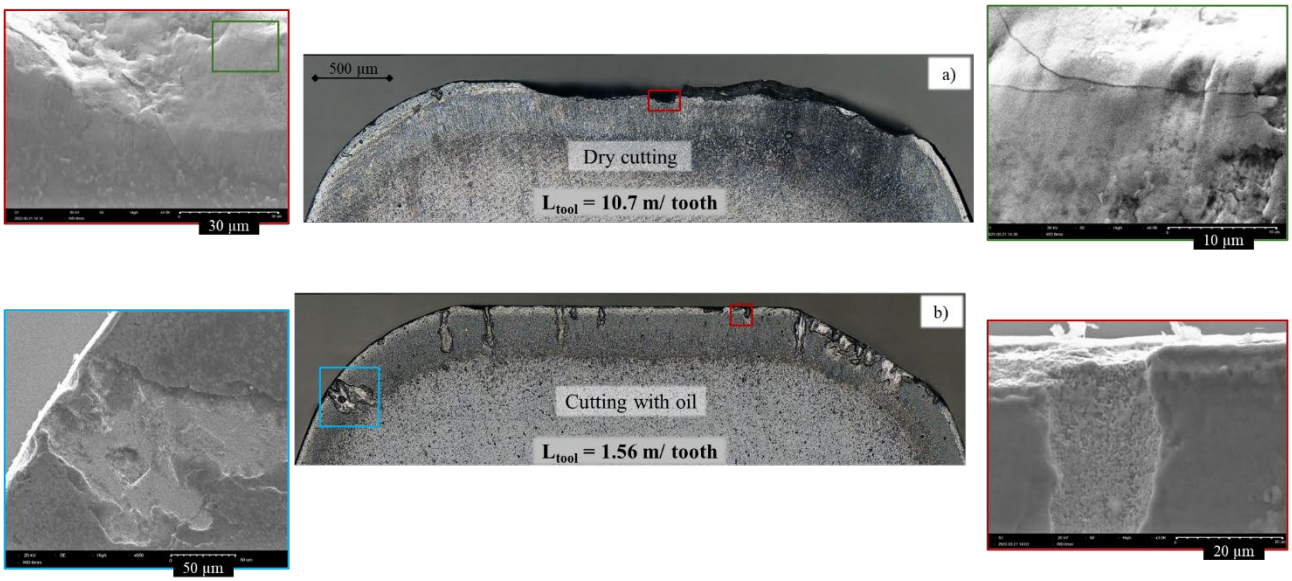

Fig. 6. Detailed wear phenomena of tungsten cemented carbide substrate cutting Q&T steel with Rm ≈ 1130 N/mm² for a) dry cutting and b) cutting with oil

Figure 7 compares the wear behavior of MC90 tool substrates during fly cutting of quenched and tempered 42CrMoS4 steel with a reduced strength level (Rm = 883 N/mm²) under dry cutting, oil lubrication, and emulsion cooling. In comparison to Figure 5, differences between oil and emulsion were observed, while dry cutting still achieves the highest tool life combined with the lowest wear level at comparable cutting lengths. Under dry cutting conditions, a relatively uniform and moderate wear progression is visible, even at extended cutting lengths of up to L_{tool} = 14.0 m/tooth.

When using oil lubrication, pronounced cutting edge chipping occurs along almost the entire cutting edge at the tip of the tooth, even at significantly lower cutting lengths. The damage is characterized by irregular edge breakouts and increased surface discoloration, indicating enhanced oxidation effects compared to both dry cutting and emulsion cooling. In contrast, machining with emulsion results in fewer cutting edge breakouts than oil lubrication; however, a distinctly different and more pronounced crater wear develops compared to dry cutting. Moreover, the location of crater

wear differs from that observed under dry conditions, indicating a modified thermo-mechanical load distribution at the rake face due to the lubricant. Despite these differences, a similar wear pattern is observed for all cutting strategies at the transition from the tip radius to the trailing flank, indicating a geometrically driven wear concentration in this region.

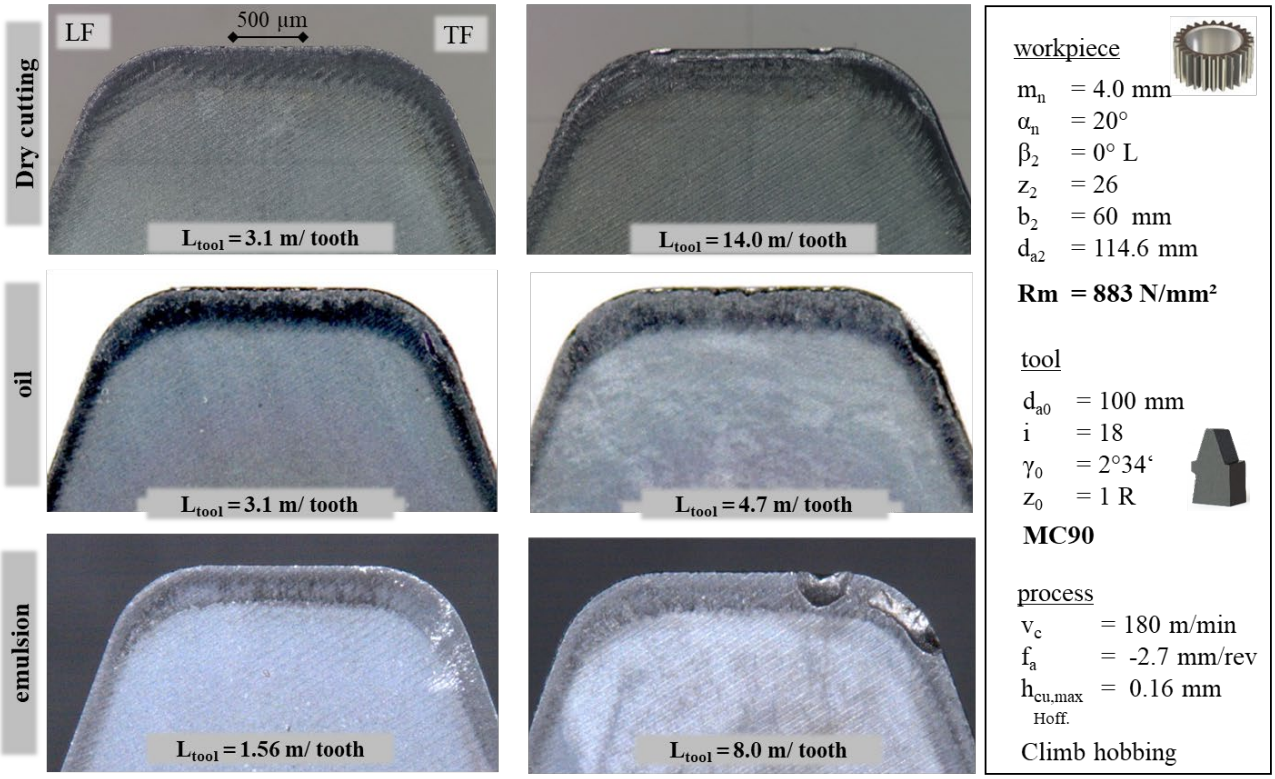

Fig. 7. Wear comparison of the of MC90 substrate cutting Q&T steel with Rm ≈ 883 N/mm²

Figure 8 compares the wear behavior obtained with PM-HSS to the previously presented results for MC90 at identical workpiece strength. Despite the reduced cutting speed, a pronounced increase in crater wear is observed when oil or emulsion are applied. For oil, crater formation occurs almost immediately and is already dominant at L_{tool} = 1.56 m/tooth, whereas for the emulsion a similar damage pattern becomes evident at L_{tool} = 6.4 m/tooth. This behavior clearly differs from dry cutting, where only minor, edge-proximal crater traces appear and only at a significantly later stage of L_{tool} = 14.0 m/tooth. The interaction between coolant and tool material responsible for this accelerated damage cannot yet be conclusively clarified. However, the change of the substrate from MC90 to PM-HSS evidently leads to fundamentally different wear patterns under lubricated conditions.

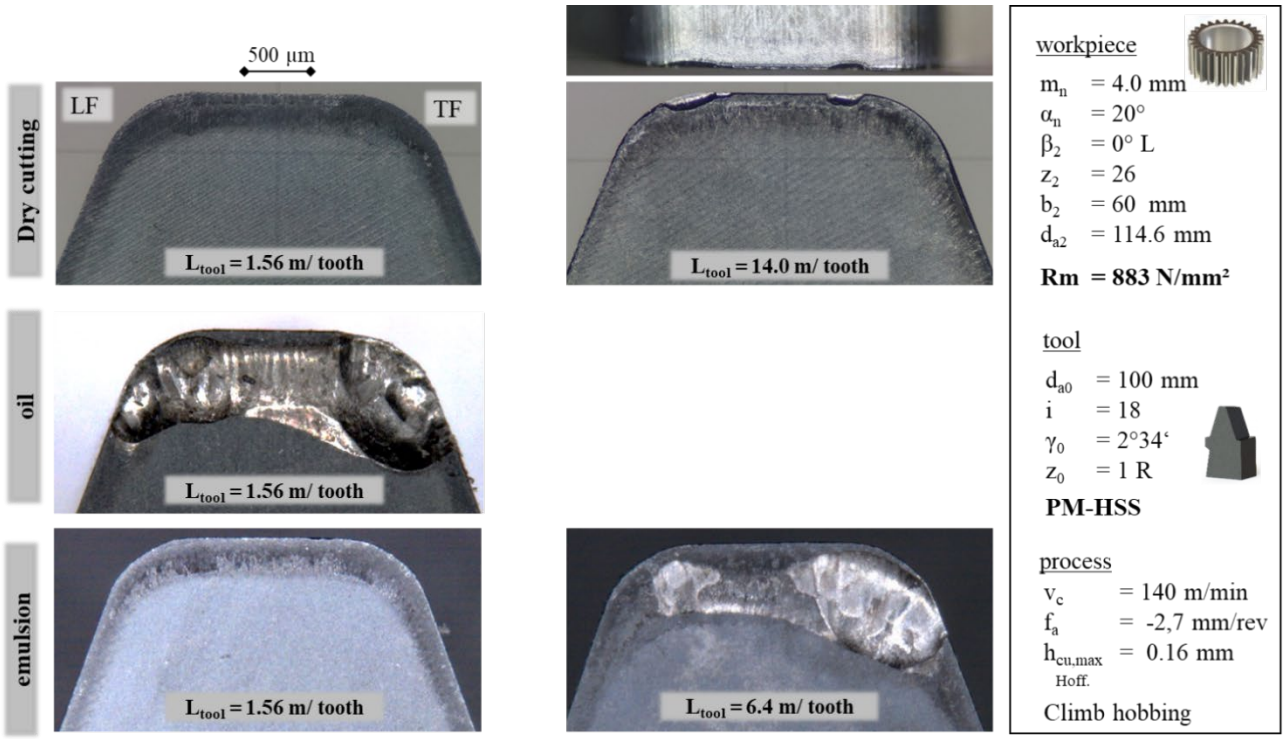

Fig. 8. Wear comparison of the of PM-HSS substrate cutting Q&T steel with Rm ≈ 883 N/mm²

Figure 9 shows the wear behavior of PM-HSS cutting tools during gear hobbing of a case-hardening steel with a tensile strength of Rm ≈ 540 N/mm², representing the lowest workpiece strength level investigated. Compared to the previously examined quenched and tempered steels, this material exhibits a distinctly different interaction with the tool substrate, resulting in a different altered wear response. Here, a similar wear behavior and comparable tool life are observed for dry cutting and oil lubrication. In both cases, tool wear is dominated by crater wear on the rake face, with similar cutting lengths of L_{tool} = 10.9 m/tooth being reached. Under oil lubrication, the crater appears slightly more washed-out and smoother compared to dry cutting, which can be attributed to the lubricating effect reducing frictional stresses at the chip–tool interface. Under dry cutting conditions, an additional crater lip breakage is observed at the transition from the tip cutting edge to the LF at L_{tool} = 10.9 m/tooth. This localized failure is not present when machining with oil, suggesting that the cooling effect of the lubricant stabilizes the crater lip and delays its detachment from the cutting edge.

A further increase in tool life is achieved when applying emulsion cooling. In this case, the achievable cutting length increases by approximately 44 %, reaching L_{tool} = 15.7 m/tooth. The images indicate a delayed initiation and slower progression of crater wear, which is attributed to the higher heat capacity of the water-based emulsion, leading to more effective heat dissipation from the cutting zone. As a result, both crater formation and propagation are delayed, extending the tool life.

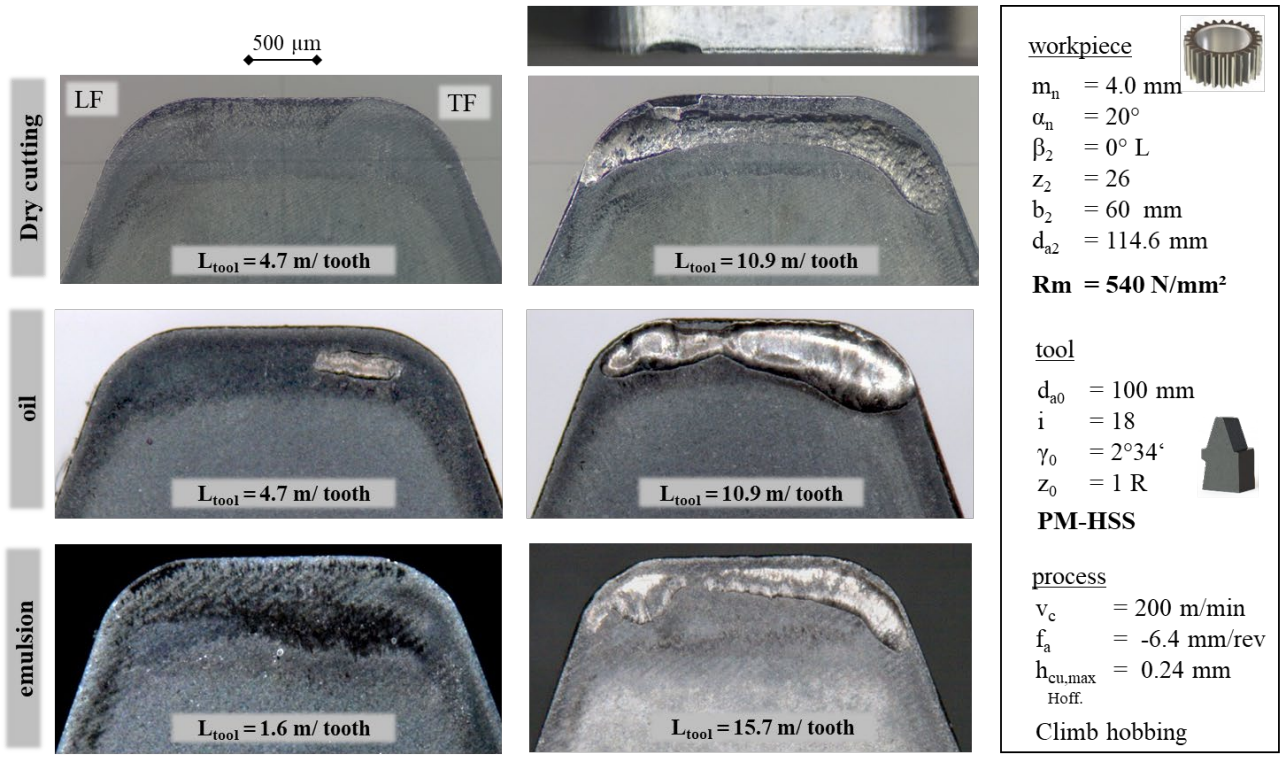

Fig. 9. Wear comparison of the of PM-HSS substrate cutting case hardening steel with Rm ≈ 540 N/mm²

Figure 10 provides a comparative and consolidated overview of all obtained tool life results and the corresponding flank wear progressions for the investigated combinations of tool substrate, workpiece strength, and coolant–lubricant strategy. The figure thus integrates the individual observations from Figures 6–10 into a unified assessment of wear behavior and process stability.

The bar chart Figure 10 d) summarizes the achievable tool life for dry cutting, oil lubrication, and emulsion cooling. In agreement with the trends observed in the preceding figures, the overall comparison clearly demonstrates a superior tool life performance under dry cutting conditions, largely independent of tool substrate and workpiece tensile strength. This advantage persists even when varying the cutting parameters and tool materials.

An exception is observed only for the machining of the case-hardening steel (Rm ≈ 540 N/mm²) using PM-HSS, where emulsion cooling achieves a higher tool life than dry cutting. This behavior is consistent with earlier investigations reported in [1] and can be attributed to the enhanced cooling effect of the water-based emulsion, which delays the initiation and progression of crater wear.

The remaining diagrams in Figure 10 a), b), c) depict the flank wear evolution for the three coolant–lubricant strategies: dry cutting (a), oil lubrication (b), and emulsion cooling (c). A comparative analysis reveals that, despite differences in cutting parameters, tool substrates, and workpiece materials, the flank wear curves under dry cutting exhibit a significantly narrower scatter band than those obtained with oil or emulsion. This indicates a more stable and predictable wear progression (process stability) for dry cutting.

In contrast, machining with oil and emulsion frequently leads to catastrophic tool failures, such as complete tool breakage or excessive edge chipping, resulting in flank wear values far exceeding acceptable limits. In these cases, tool reconditioning or reliable continuation of the process is no longer feasible, rendering such process variants economically and technologically unsuitable. Only the PM-HSS tool machining the low-strength workpiece steel (Rm ≈ 540 N/mm²) exhibits a stable wear progression under coolant application.

Overall, Figure 10 confirms that, even when reducing workpiece tensile strength or changing the tool substrate, dry cutting provides the most favorable and robust wear behavior for gear hobbing of quenched and tempered steels with progressive cutting parameters. Whether the cooling action of oil and emulsion induces thermally driven damage mechanisms, such as substrate thermal shock,

particularly for high-strength Q&T steels, could not be conclusively clarified within the present study. While such behavior is well documented for cemented carbides, comparable effects for MC90 and PM-HSS substrates have not yet been conclusively reported and require further investigation.

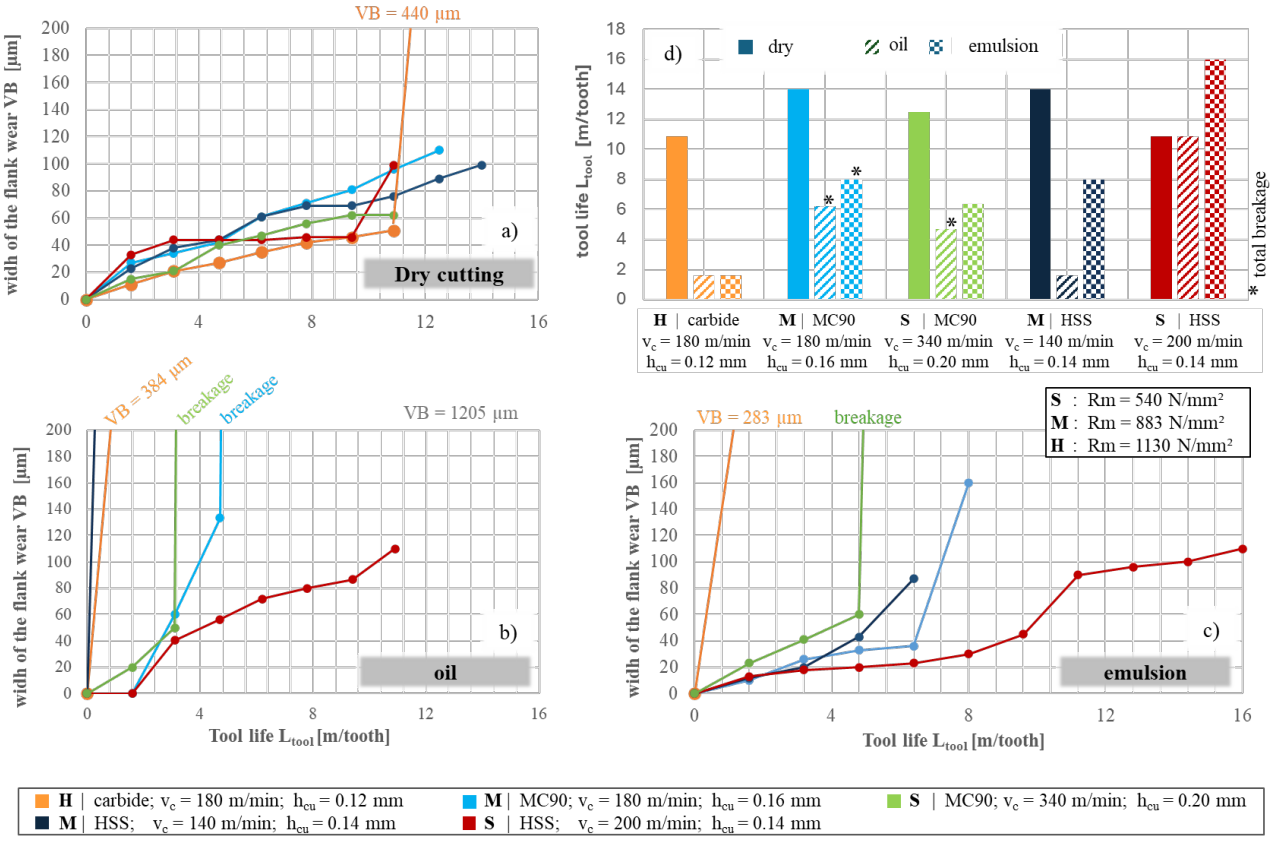

Fig. 10. a),b),c) Resulting flank wear using different coolant strategies d) Tool life comparison for different cutting conditions

Conclusion

In this paper investigations on the influence of cooling and lubrication strategies (dry cutting, oil, and emulsion) on tool wear and tool life in gear hobbing using different tool substrates (MC90, PM-HSS) and workpiece materials with varying tensile strength (Rm ≈ 540–1130 N/mm²) were shown.

Across all investigated tool–workpiece combinations, dry cutting shows the most robust and reproducible tool life behavior, particularly for high-strength steels. Compared to oil and emulsion, dry cutting exhibits narrower scatter in flank wear progression and a lower tendency for severe crater wear, edge chipping, or premature tool breakage.

An exception is observed for PM-HSS machining of the low-strength case-hardening steel (Rm ≈ 540 N/mm²), where emulsion provides a tool life increase of up to 44 %, attributed to its superior cooling capacity delaying crater wear initiation.

Overall, the results demonstrate that dry gear hobbing with these parameters is a technically and economically favorable strategy for high-strength steels, while the use of cooling lubricants may induce unstable wear mechanisms. The role of thermally induced damage under lubricated conditions requires further investigation.

Acknowledgements

This project was funded by the VDW Research Institute.

References

[1] Forschungsvereinigung Antriebstechnik e.V.: Leistungspotentiale des Kühlschmierstoffeinsatzes beim Wälzfräsen. FVA-Forschungsheft Nr. 1278, Frankfurt, 2018

[2] Cselle, T.: Trockenbearbeitung beim Wälzfräsen. Tagungsband zum Seminar „Trockene Zahnradvorbereitung“, Aachen, 15.-16.02.2002, ADITEC, 2002

[3] Kleinjans, M.: Wälzfräsen am Limit. Tagungsband zum Seminar „Trockene Zahnradvorbereitung“, Aachen, 15.-16.02.2002, ADITEC, 2002

[4] Forschungsvereinigung Antriebstechnik e.V.: Bearbeitung extrem schwefelarmer Stähle durch Bohren und Wälzfräsen. FVA-Forschungsheft Nr. 948, Frankfurt, 2010

[5] Karpuschewski, B.; Beutner, M.; Köchig, M.; Wengler, M.: Cemented carbide tools in high speed gear hobbing applications. CIRP Annals – Manufacturing Technology 66 (2017) S. 117-120, https://doi.org/10.1016/j.cirp.2017.04.016

[6] Klocke, F., Kauffmann, P., Schalaster, R., Stuckenberg, A.: Comparison of PM-HSS and Cemented Carbide Tools in High-Speed Gear Hobbing. Gear Technol. 09/10 (2009) S. 57-59

[7] Sari, D.; Troß, N.; Löpenhaus, C.; Bergs, T.: Development of an application-oriented tool life equation for dry gear finish hobbing. Wear 426-427 B (2019) S. 1563-1572, https://doi.org/10.1016/j.wear.2018.12.037

[8] Bausch, T.: Innovative Zahnradfertigung. 5. Auflage, Expert Verlag, Renningen 2015, ISBN 978-3-8169-3280-2

[9] Kühn, F., Hendricks, S., Troß, N. et al. Experimental analysis on the influence of the tool micro geometry on the wear behavior in gear hobbing. Int J Adv Manuf Technol 126, 1279–1292 (2023). https://doi.org/10.1007/s00170-023-11158-x

[10] Karpuschewski, B., Knoche, H.-J., Hipke, M., Beutner, M. High Performance Gear Hobbing with powder-metallurgical High-Speed-Steel, Procedia CIRP, Vol. 1, 2012, pp. 196-201, https://doi.org/10.1016/j.procir.2012.04.034.

[11] Weck, M.; Hurasky-Schönwerth, O.; Winter, W., M. Manufacturing simulation for the analysis of the gear hobbing process, In: International Conference on Gears, March 13 - 15, 2002 / VDI-Gesellschaft Entwicklung Konstruktion Vertrieb, pp. 145-159., 2002

[12] Weck, M., Klocke, F., Winter, W., & Winkel, O. Analysis of Gear Hobbing Processes by Manufacturing Simulation Production Engineering. In Research and Development. WGP Berlin, 2003

[13] Karpuschewski, B., Beutner M., Köchig M., Wengler M. Cemented carbide tools in high speed gear hobbing applications, CIRP Annals,Volume 66, Issue 1, 2017, Pages 117-120, https://doi.org/10.1016/j.cirp.2017.04.016

[14] Schalaster, R., Optimierung des Fertigwälzfräsens von Verzahnungen. Ph.D. Thesis, RWTH Aachen University, Aachen, 2012.